Hypomyelination of interneurons in the APO-SUS rat model for schizophrenia

Noor van Vugt[1, 2]

Supervisors: Dorien Maas[1, 2, 3], Gerard Martens[1], and Brahim Nait-Oumesmar[2]

Second reader: Marcia Spoelder[3]

[1] Department of Molecular Animal Physiology, Radboud Institute for Molecular Life Sciences, Radboudumc, Radboud University Nijmegen, the Netherlands

[2] Department of Myelin Plasticity and Regeneration, Institut du Cerveau et de la Moelle épinière, Paris, France

[3] Department of Cognitive Neuroscience, Donders Centre for Medical Neuroscience, Radboudumc, Radboud University Nijmegen, the Netherlands

Master internship report

Noor van Vugt

S1011705

Plasticity & Memory

Cognitive Neuroscience

Radboud University Nijmegen

Internship period: September 2018 – July 2019

Abstract

Schizophrenia is a neurodevelopmental disorder that affects about 0,5% of the world population. Symptoms can be categorized into positive, negative, and cognitive clusters. Although most research and treatment currently is focused on the positive symptoms (such as hallucinations), cognitive symptoms represent another core feature of the disorder. The current study investigates the neurobiological mechanism underlying cognitive symptoms of schizophrenia by using the APO-SUS rat model for schizophrenia. Using electron microscopy, we found that the prefrontal cortex (PFC) of APO-SUS rats contains fewer myelinated axons than the PFC of APO-UNSUS rats. This effect is normalized by environmental enrichment of the home cages of the APO-SUS rats. Additionally, using immunofluorescence on 70 nm ultrathin slices of PFC, we were able to visualise individual myelin sheaths and intra-axonal GABA, allowing us to quantify the density of myelinated interneurons. We found that in APO-SUS PFC a lower percentage of myelinated axons was GABAergic than in APO-UNSUS PFC. Together, these data show that in the APO-SUS rat model for schizophrenia interneurons are subject to hypomyelination, and that this defect can be rescued by environmental enrichment.

Keywords*: schizophrenia, APO-SUS rats, myelin, hypomyelination, G-ratio, interneurons*

Introduction

Schizophrenia (SZ) is a psychiatric disorder characterized by positive symptoms (e.g. delusions and hallucinations), negative symptoms (e.g. loss of social and affectional abilities), and cognitive symptoms (e.g. deficits in executive functioning, memory, and attention) which affects approximately 0,5% of the world population (Saha et al., 2005). SZ is associated with several adverse functional outcomes, like substance use, self-harm, homelessness and unemployment (Kooyman et al., 2007), and although there are antipsychotic and behavioural treatments, these are not effective for all patients and all symptoms. The current treatment methods mainly focus on the positive symptoms, while it has been found that cognitive dysfunction is also a core feature of the disorder. Premorbid cognitive deficits are a risk factor for developing SZ (Reichenberg et al., 2010; 2006a; 2006b), and cognitive impairment is critically related to functional outcome of the disorder (Green, 2006), thus making the cognitive symptoms an appealing target for treatment.

Cognitive symptoms of SZ cover a wide range of cognitive functions, like attention, planning, working memory, and behavioural and emotional self-regulation. How and to which extent these symptoms present themselves differs from patient to patient, but deficits in executive functioning are observed in most patients (Orellana & Slachevsky, 2013). Impairments in executive functioning in SZ are thought to arise from alterations in the dorsolateral prefrontal cortex (DLPFC) (Orellana & Slachevsky, 2013), and two neurobiological features in this area are hypothesised to play a role in the development of these symptoms. The first of these two features is decreased myelination of axons (Maas et al., 2017; Stedehouder & Kushner, 2017). SZ patients show reduced white matter (WM) integrity in frontal circuits relative to healthy controls (Breier et al., 1992; Buchanan et al., 1998; Fitzsimmons et al., 2013; Kubicki et al., 2005; Kuswanto et al., 2012), which has been associated with the cognitive symptoms of the disorder (Karlsgodt et al., 2008; Qiu et al., 2009). WM alterations can be caused by several factors, including axonal loss and myelin abnormalities. Imaging methods that are sensitive to the detection of myelin have suggested that myelin abnormalities are the most probable cause of this (Chang et al., 2017; Scheel et al., 2013). This hypothesis is supported by the fact that SZ onset usually coincides with the peak of myelin development of the PFC during young adulthood, while effects of axonal abnormalities should be observable earlier during development.

Accordingly, rodent models of SZ show decreased WM volume, abnormal myelin sheath morphology, and downregulation of several myelin-related proteins, which were associated with cognitive impairments similar to those observed in SZ patients (Filiou et al., 2012; Rosenbluth & Bobrowski-Khoury, 2013; Xiu et al., 2014). Moreover, analysis of *post-mortem* brain tissue of SZ patients reveals reduced expression of myelin-related mRNAs (Hakak et al., 2001; Haroutunian et al., 2006) and oligodendrocyte (OL)-related mRNAs. OLs are glial cells in the brain that produce myelin and it has been shown that genetic variants of OL-related genes are associated with WM tract integrity and cognitive impairments in both healthy controls and SZ patients (Prata et al., 2013; Voineskos et al., 2012). Studies of *post-mortem* tissue of SZ patients have found a reduced density of OLs (Hof et al., 2002; Vostrikov et al., 2004), and reduced expression of OL-related protein in frontal cortical areas (Flynn et al., 2003). These findings suggest impaired OL functioning as a cellular mechanism underlying reduced myelination in SZ patients.

The second mechanism thought to underlie cognitive symptoms in SZ is dysfunction of interneurons (Benes et al., 1991; Do et al., 2015), which is mainly apparent through impaired inhibitory neurotransmission. Studies have found decreased expression of GAD67, the synthesizing enzyme of GABA, in SZ patients relative to controls (Akbarian et al., 1995; Lewis, 2009; Volk et al., 2000), specifically in the parvalbumin (PV)-positive subclass of GABAergic interneurons (Hashimoto et al., 2003). Moreover, PV mRNA and protein are less expressed in *post-mortem* tissue of schizophrenic patients (Hashimoto et al., 2003; Lewis, 2009), indicating impaired functioning of PV-positive interneurons in PFC. PV basket cells are crucial for neuronal synchronization at the gamma-band frequency through phasic inhibition of pyramidal neurons in the PFC (Kann et al., 2014; Lewis et al., 2012). This synchronization is essential for cognitive functioning, and accordingly impairment in this synchronization is associated with cognitive impairment in SZ patients (Gonzalez-Burgos et al., 2015; Gonzalez-Burgos & Lewis, 2008). Moreover, the PV interneuron subclass is the main type of interneuron that is myelinated in the cortex (Micheva et al., 2016; 2018). The exact function of this myelin is not known yet, but it could be related to the tuning of conduction velocity of the action potentials to allow for synchronous arrival at the synapse, irrespective of the distance to be travelled, similar to the mechanism in excitatory axons (Micheva et al., 2018; Pajevic et al., 2014; Stedehouder & Kushner, 2017). For PV interneurons specifically, myelination of the axons could be additionally related to their high metabolic demand due to their high spiking rate and long dendrites, which are features that are not shared with other subclasses of interneurons (Stedehouder & Kushner, 2017). Several studies have therefore hypothesized that altered myelination of PV interneurons is a probable locus of neurobiological pathophysiology underlying cognitive deficits in SZ (Maas et al., 2017; Stedehouder & Kushner, 2017).

We used the apomorphine-susceptible (APO-SUS) rat model for schizophrenia. This model is developed by Ellenbroek et al. (1995) and shows a high construct validity for SZ relative to other SZ rodent models. APO-SUS rats show similarities to SZ patients in the cognitive domain by displaying impaired spatial working memory, reduced pre-pulse inhibition and latent inhibition, and impaired cognitive flexibility in the extra-dimensional set-shifting task (Ellenbroek et al., 1995; Maas et al., unpublished data), which are functions associated with the medial PFC (mPFC; corresponding to human DLPFC). Additionally, this rat model shows central nervous system, endocrinological, and immunological similarities to SZ patients (Ellenbroek et al., 1995), making it an interesting nonpharmacological animal model for SZ. The apomorphine-unsusceptible (APO-UNSUS) rat is the phenotypic counterpart of the APO-SUS rat. These two lines originate from a selective breeding procedure where rats with a “high” gnawing response to apomorphine injection are bred together to form the APO-SUS line, and likewise rats with a “low” gnawing response are bred together to form the APO-UNSUS line (for definition of “high” and “low” gnawing response, see Ellenbroek et al., 1995). Additionally, it has been found that multisensory enrichment of the home cage (environmental enrichment; EE) restores cognitive flexibility in the APO-SUS rat model (Maas et al., unpublished data), and similarly that exercise alleviates symptomatology in SZ patients (Mittal et al., 2017). Moreover, rodent studies have shown that exercise and social engagement positively influence myelination (Tomlinson et al., 2016; Yang et al., 2013), making it probable that EE of the home cages will also increase myelination in the mPFC of our APO-SUS rats.

To test the hypotheses that interneurons are less myelinated in SZ PFC, and that EE has a positive effect on myelination of axons, we assessed both the density and the integrity of

myelinated axons in the APO-SUS mPFC with electron microscopy and immunofluorescence staining on ultrathin tissue sections. We found that APO-SUS rats have significantly less myelinated axons in the mPFC as compared to APO-UNSUS rats, but that the integrity of the myelin sheaths is normal. EE normalises the density of myelinated axons of APO-SUS rats to some extent. Moreover, we found a reduced proportion of myelinated interneurons in APO-SUS rats as compared to APO-UNSUS rats.

Methods

Experimental animals

Samples used were brains from naive male APO-SUS and APO-UNSUS rats. Rats were kept in a 12 hour light-dark cycle (lights on at 7:00) and had ad libitum access to water and standard laboratory chow. They were kept in eurostandard type III cages in pairs. All rats were bred and housed in the central animal facility of Radboud University Nijmegen, the Netherlands and all experiments described here were approved by the Animal Ethics Committee of Radboud University Nijmegen, and conducted according to Dutch legislation. The animals were sacrificed at PND21 or PND90 through transcardial perfusion with 2% PFA/2% glutaraldehyde, after which their brains were extracted, post fixed overnight in 2% PFA/2% glutaraldehyde and kept in PB with 0.01% azide until further processing.

Environmental enrichment

Environmental enrichment was performed during a previous experiment in our laboratory, and brains from this experiment were used in the current study. Environmental enrichment methods were as follows: Half of both the APO-SUS and APO-UNSUS rats were kept in standard housing, and the other half was kept in environmentally enriched cages from PND21 onwards. The EE cage was 100 x 54,5 x 48 cm, and rats were housed in groups of 10. The cage was further enriched by objects such as toys, running wheels, nesting places, and tunnels, promoting cognitive stimulation, social interaction, and novelty exploration. The enrichment objects were changed three times a week to encourage exploration. Rats in environmentally enriched cages were kept in the same room as rats in standard housing.

Electron microscopy

APO-SUS and APO-UNSUS rats, both with and without having undergone environmental enrichment, were sacrificed at PND90 and their brains were extracted. Left hemispheres were cut on a vibratome (Leica VT 1000S) into 100 µm thick sagittal sections. These sections were stored in 0.1 M PB/0,01% azide at 4 °C until further use. The most lateral section containing PFC (figure 81 Paxinos and Watson Rat Brain Atlas) was selected for further processing and prelimbic (PL) and infralimbic (IL) subareas of the mPFC were isolated and processed separately. Sections were incubated for 30 minutes in 2% Osmium Tetroxide solution. After two ten-minute washes in Milli-Q water, they were put in filtered 5% Uranyl Acetate for 30 minutes, and then washed again three times for 10 minutes in Milli-Q. Dehydration was achieved by putting the sections sequentially 2 x 5 minutes in 25% ethanol, 2 x 5 minutes in 50% ethanol, 1 x 5 minutes in 70% ethanol and a second time in 70% ethanol overnight. The next day dehydration was continued with 2 x 5 minutes in 95% ethanol, and 3 x 20 minutes in 100%

ethanol. After dehydration, sections were put in pure acetone for 15 minutes, and then in a 1:1 mixture of acetone and epon resin for 1 hour. Sections were then transferred to pure epon resin and incubated overnight. The following day, the sections were included between two glass slides with epon and polymerized at 60 °C for 48+ hours. Sections were cut on the ultramicrotome (Leica EM UC7) into ultrathin (70 nm) sections and mounted on copper grids. Subsequently, after a short rehydration step in Milli-Q, the grids were placed in lead citrate (Electron Microscopy Sciences) for 7-10 minutes in the presence of sodium hydroxide to absorb CO_2, and finally washed 4 x 2 minutes in Milli-Q. A transmission electron microscope (Hitachi HT7700, operating at 100 kV) was used to image the sections. Electron micrographs were taken with an integrated AMT XR41-B camera (2048 x 2048 pixels) at a magnification of 26.000 x in layer 5 of the neocortex, at a distance of approximately 300 µm from the outer edge of the corpus callosum. Per sample, 40 non-overlapping images were taken, which were analysed with ImageJ.

LRWhite embedding for immunofluorescence

APO-SUS and APO-UNSUS rats reared in standard housing were sacrificed at PND90 and their brains were extracted. Left hemispheres were sliced into 100 µm thick sagittal sections on the vibratome (Leica VT 1000S) and stored in 0.1 M sodium cacodylute/0.1 M $CaCl_2$ at 4 °C. The IL area was isolated from the most lateral section containing PFC (figure 81 Paxinos and Watson Rat Brain Atlas) of each brain and processed further separately. For embedding in LRWhite resin, tissue sections were first dehydrated by putting them sequentially in 50%, 70%, 80%, 90%, and 95% ethanol, each for 15 minutes. They were then transferred to LRWhite resin (Hard Grade; London Resin Company Limited) and incubated for one hour at room temperature in the dark, then put in fresh LRWhite resin and left for another hour. They were then put in fresh LRWhite again and left for 12 hours at room temperature and in the dark. After 12 hours the sections were transferred to gelatine capsules which were filled with LRWhite and closed off air-tight, and were then left to polymerize at 60 °C for 2-3 days. Solid LRWhite blocks were cut on the ultramicrotome (Leica EM UC7) into ultrathin (70 nm) sections and mounted on gelatine-coated glass slides. The slides were left to dry on a hot plate (100 °C) for 30 minutes.

Immunofluorescence on ultrathin LRWhite-embedded sections

Sections were blocked against auto-fluorescence with 100 mM glycine in Milli-Q for five minutes. After washing with PBS, the primary antibody was applied and left to incubate overnight at 4 °C. Primary antibodies used are anti-MBP chicken (MBP, Aves, 1:200) and anti-GABA guinea-pig (AB175, Millipore, 1:500), dissolved in 2% BSA in 1x PBS. Due to the ultrathin slices, antibodies were able to penetrate into the axons, and intra-axonal GABA could be visualised. After overnight incubation and washing with PBS, secondary antibodies were applied to incubate for 30 minutes at room temperature. Secondary antibodies used were IgG anti-chicken (Alexa 594, 1:150), IgG anti-guinea pig (Alexa 488, 1:150), and DAPI (1:1000), dissolved in 1% BSA in 1x PBS. After washing with PBS, coverslips were added with fluoromount (Thermo Fischer Scientific), and the slides were stored at 4 °C. A fluorescence microscope (Zeiss Axio-Imager M2) with ApoTome (Apotome.2) was used to image the slices. Images were taken with an AxioCam MRm camera, using ZEN software (Blue edition). The entire section was imaged at a magnification of 63x (oil immersion lens) with the FITC and TRITC channels.

Immunofluorescence for BCAS1

Right hemispheres of APO-SUS and APO-UNSUS animals sacrificed at PND21 and PND90 were cut coronally on the cryostat (Leica) and stored at -20 °C until further use. After rehydration of the slices and one hour incubation in 4% BSA, sections containing PFC (figure 10 Paxinos and Watson Rat Brain Atlas) were stained with BCAS1 primary antibody (anti-NABC1, Abcam, PND21 1:500, PND90 1:100) and left to incubate overnight at 4 °C. The secondary antibodies IgG anti-rabbit (Alexa 488, 1:1000) and DAPI (1:1000) were added after washes with 1x PBS and incubated for two hours at room temperature. The secondary antibody was washed off with 1x PBS/0,1% Triton, and coverslips were attached with fluoromount (Thermo Fisher Scientific).

Statistics

Statistical tests were performed in IBM SPSS Statistics 26. One-way ANOVA's were applied to electron microscopy data and two-tailed independent samples T-tests were applied on immunofluorescence data. *P*-values < 0,05 were considered statistically significant, *p*-values < 0,1 are considered a trend. Data are presented as mean ± standard error of the mean (SEM), unless indicated otherwise.

Results

Lower density of myelinated axons in APO-SUS rats

Both the density of myelinated axons and the integrity of the myelin sheaths in APO-SUS and APO-UNSUS rats with and without EE was analysed. Electron microscopy images were analysed for the number of myelinated axons per image. Together with the surface area of the image, this resulted in an average number of myelinated axons per mm^2 for each brain (IL: $M = 23344$, $SD = 10048$, PL: $M = 17097$, $SD = 5335$). A one-way ANOVA showed a non-significant difference between the four groups in number of myelinated axons per mm^2 for both IL and PL (IL: $F(3, 10) = 3.14$, $p = .074$; PL: $F(3, 11) = 3.12$, $p = .070$). However, for both areas a trend was found ($p < .1$), and subsequent independent samples T-tests were performed to see where this trend originated from. A Tukey post-hoc test would be too conservative in this case since it compares all groups and corrects consequently for a large number of comparisons. With the independent samples T-tests, we only compared the groups that were of interest to our research question, making it more sensitive to detect differences. T-tests were done between APO-SUS and APO-UNSUS groups, APO-SUS and APO-SUS EE groups, and APO-SUS EE and APO-UNSUS groups. In IL, the APO-UNSUS group showed a significantly higher number of myelinated axons per mm^2 than the APO-SUS group (135% increase; Figure 1B; $t(5) = -2.80$, $p = .038$). In PL, a similar comparison showed that APO-UNSUS animals contain 64% more myelinated axons per mm^2 than APO-SUS animals, but the difference did not reach significance ($t(5) = -2.19$, $p = .080$). The T-tests between APO-SUS and APO-SUS EE, and APO-SUS EE and APO-UNSUS did not indicate significant differences in both IL and PL.

APO-SUS rats have normal myelin integrity

To assess the integrity of the myelin, the G-ratio of each myelinated axon was calculated as the average diameter of the axon alone along the two main axes (axon calibre) divided by the average diameter of the axon including myelin over the same two axes (myelin calibre; see Figure 1C). A typical G-ratio in the cortex lies around 0,7 (Fraher & Dockery, 1998; Yang et al., 2013), where a lower value represents thicker myelin, and a higher value represents thinner myelin. We found a significant positive correlation between axon calibre and G-ratio for all groups (see Figure 1D; four separate linear regression analyses were performed, APO-SUS: $F(1, 192) = 161.76$, $p < .01$, APO-SUS EE: $F(1, 267) = 196.41$, $p < .01$, APO-UNSUS: $F(1, 298) = 241.99$, $p < .01$, APO-UNSUS EE: $F(1, 344) = 297.49$, $p < .01$), indicating that the normal pattern of thicker myelin on thinner axons and thinner myelin on thicker axons could be observed in our data. This shows that the quality of myelin is normal across all axon calibres in each group. Additionally, the mean G-ratios of the four groups were compared with one-way ANOVA in IL and PL separately. These tests showed that in IL, mean G-ratio does not differ across groups (Figure 1E; $F(3, 10) = 1.62$, $p = .246$) but in PL a significant effect of group on the mean G-ratio was found ($F(3, 11) = 4.01$, $p = .037$). A subsequent T-test revealed a significantly higher G-ratio, and thus thinner myelin in APO-SUS versus APO-UNSUS animals ($t(5) = 3.14$, $p = .026$).

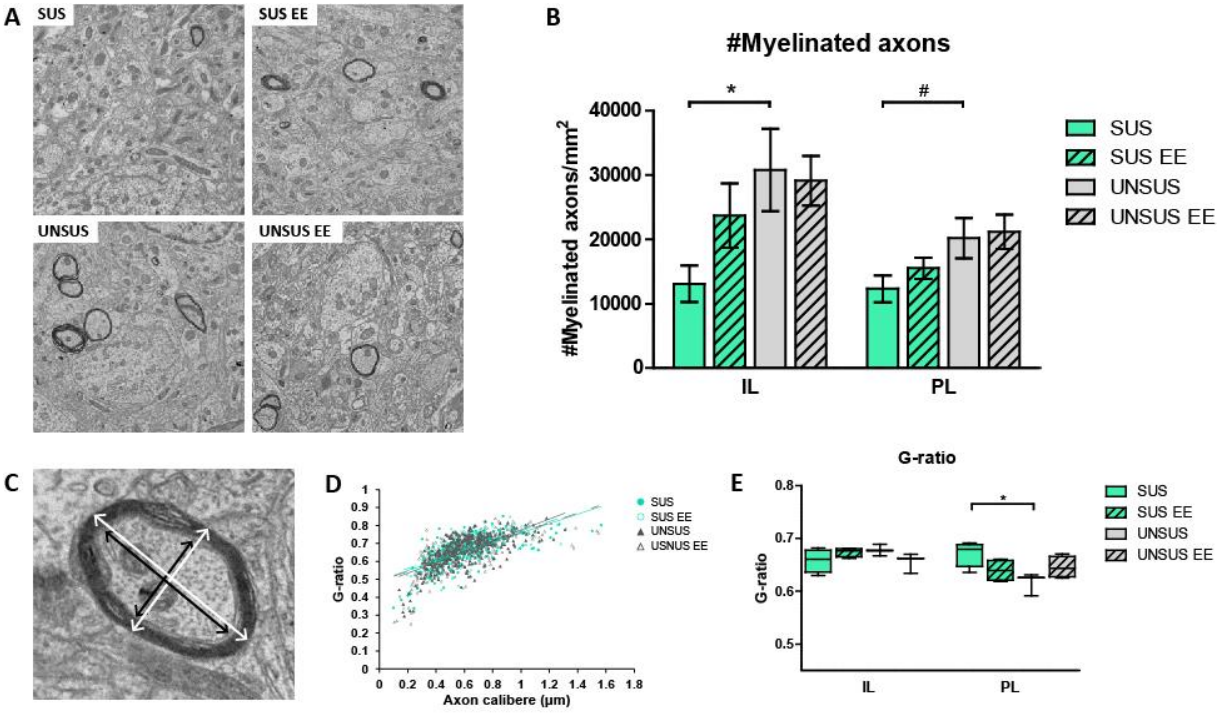

Figure 1. Assessment of myelin density and integrity in mPFC of APO-SUS and APO-UNSUS rats with standard housing and EE. (A) Transmission electron microscope images of rat mPFC. Dark circles are myelin sheaths around axons. (B) Quantification of number of myelinated axons per mm², counted in IL (APO-SUS n = 4, APO-SUS EE n = 4, APO-UNSUS n = 3, APO-UNSUS EE n = 3) and PL (APO-SUS n = 4, APO-SUS EE n = 4, APO-UNSUS n = 3, APO-UNSUS EE n = 4) separately. Bars represent group mean ± SEM. (C) Zoomed image of one myelinated axon. Axon calibre is calculated as the average of the lengths of the two black arrows. Myelin calibre is the average of the lengths of the two white arrows. G-ratio is calculated as axon calibre divided by myelin calibre. (D) G-ratio of each individual axon plotted against its axon calibre. Lines represent linear trends per group. (E) Boxplots of average G-ratio per group, measured in IL and PL separately. Boxes represent the first until the third quartile of the data, whiskers depict minima and maxima. *: $p < .05$; #: $p < .1$.

Hypomyelination occurs in all axon sizes

As we found a lower number of total myelinated axons in APO-SUS than APO-UNSUS PFC, we next investigated whether the axon calibre distributions of the groups differed accordingly. We counted the average number of axons per brain in each axon calibre category for all groups. Using an independent samples Kolmogorov-Smirnov test, we checked if the distributions were different between pre-specified groups. This test analyses if there is a difference in shape and/or location between two distributions. Since only pairwise comparisons can be made, we looked at APO-SUS versus APO-UNSUS, APO-SUS versus APO-SUS EE, and APO-SUS EE versus APO-UNSUS groups. In all three comparisons no significant difference was found between the distributions for both IL and PL (Figure 3; APO-SUS vs APO-UNSUS IL: $D(271) = 0.74$, $p = .649$, PL: $D(223) = 0.18$, $p = 1.000$; APO-SUS vs APO-SUS EE IL: $D(254) = 0.34$, $p = 1.000$, PL: $D(209) = 0.37$, $p = .999$; APO-SUS EE vs APO-UNSUS IL: $D(339) = 0.93$, $p = .348$, PL: $D(230) = 0.53$, $p = .942$), suggesting that hypomyelination occurs on axons of all sizes, rather than only on axons of a specific size.

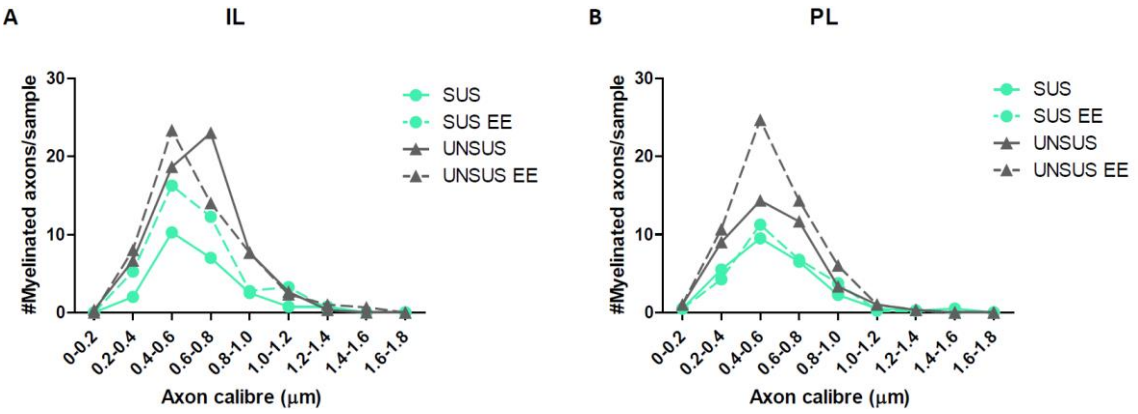

Figure 2. Distributions of number of myelinated axons in each axon calibre category per brain. (A) Number of myelinated axons in each category per brain in IL. (B) Number of myelinated axons in each category per brain in PL.

Interneurons are hypomyelinated in APO-SUS vs APO-UNSUS PFC

Since hypomyelination of APO-SUS PFC was not attributable to axon size, our next step was to investigate whether the difference in PFC myelination between APO-SUS and APO-UNSUS could be explained on the basis of the neuronal subgroup to which the axons belonged. Specifically the GABAergic interneurons were of interest. In fluorescent images of ultrathin slices of rat IL mPFC, the numbers of myelinated (MBP-positive) axons, and GABAergic myelinated (GABA- and MBP-positive) axons per mm^2 were quantified. Additionally, the average proportion of GABAergic myelinated axons out of the total number of myelinated axons was calculated per experimental group. Independent samples T-tests were performed to test for differences between APO-SUS and APO-UNSUS in mean myelinated axon density, mean GABAergic myelinated axon density, and mean percentage of myelinated axons containing GABA. One outlier in the APO-SUS group was excluded from analysis. These tests showed that there are no significant differences in both myelinated axon density (Figure 4B; $t(4) = -1.53$, $p = .201$) and GABAergic myelinated axon density ($t(4) = -2.05$, $p = .110$). We did find a significantly higher proportion of GABAergic axons

out of the total number of myelinated axons in APO-UNSUS relative to APO-SUS animals (57% increase; Figure 4C; $t(4) = -3.69$, $p = .021$).

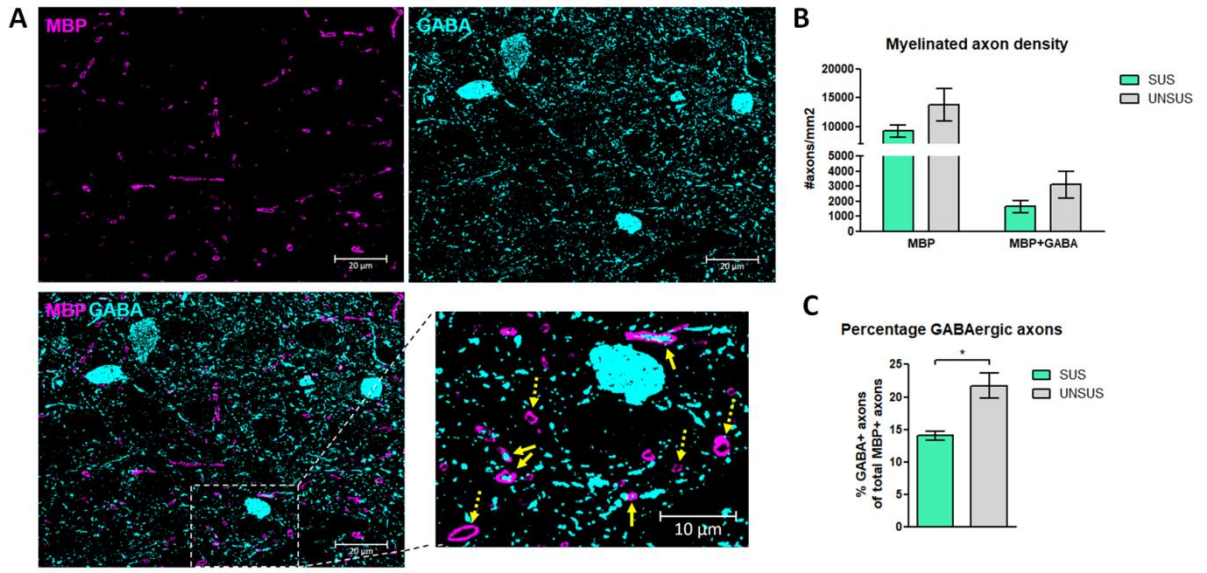

Figure 3. Quantification of GABAergic myelinated axons. (A) Immunofluorescent images of 70 nm ultrathin slices of rat IL mPFC. In violet are MBP-positive myelin sheaths, and in blue is GABA. GABAergic axons are where GABA is present inside the myelin sheath. The fourth image is a zoomed image of the rectangle indicated in the third image. Dashed arrows indicate non-GABAergic myelinated axons, solid arrows indicate GABAergic myelinated axons. Scale bars in the first three images correspond to 20 µm, scale bar in the last image corresponds to 10 µm. (B) Quantification of number of myelinated axons (MBP) and GABA-positive myelinated axons (MBP+GABA) per mm^2 for APO-SUS (n = 4) and APO-UNSUS (n = 3). (C) Percentage of total number of myelinated axons that contain GABA for APO-SUS and APO-UNSUS. *: $p < .05$.

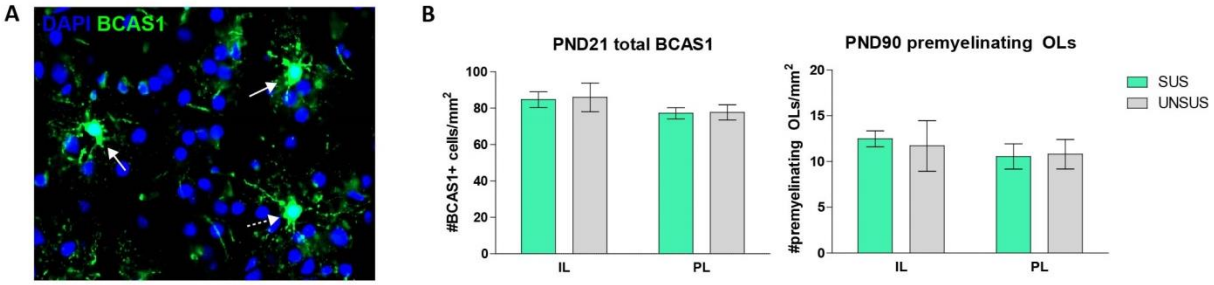

Figure 4. Quantification of BCAS1-positive cells in rat mPFC. (A) Immunofluorescence image of rat mPFC, stained for BCAS1-positive cells in green, and cell nuclei stained with DAPI in blue. Premyelinating OLs have radial processes and are indicated with solid arrows, the dashed arrow indicates an OL in an early myelinating stage. (B) The density of all BCAS1-positive cell bodies that co-localised with a DAPI stained nucleus was quantified for PND21 (APO-SUS n = 8, APO-UNSUS n = 8) in IL and PL separately. In PND90, only the premyelinating OLs (solid arrows) were quantified (APO-SUS n = 7, APO-UNSUS n = 7), in IL and PL separately.

No difference in early myelinating OL density

In view of our finding of hypomyelination with normal G-ratio, we wanted to test the hypothesis that the observed hypomyelination stems from a dysfunction of myelinating oligodendrocytes. We stained PFC slices of both adolescent (PND21) and adult (PND90) rats with an antibody

against BCAS1. The BCAS1-protein is present in an early myelinating subpopulation of OLs, but is also expressed in the premyelinating stage of OL development (Fard et al., 2017). We quantified the total density of BCAS1-positive cells in IL and PL separately in PND21 brains. Independent samples T-tests showed that no significant differences were present in the density of BCAS1-positive cells between APO-SUS and APO-UNSUS PFC (IL: $t(14) = -0.14$, $p = .890$, PL: $t(14) = -0.10$, $p = .919$). The premyelinating stage of OL development can be distinguished from other BCAS1-positive cells by the presence of processes extending symmetrically and radially from the cell body (Fard et al., 2017). In PND90, we quantified only these premyelinating OLs. We found no significant difference in the number of premyelinating OLs between APO-SUS and APO-UNSUS PFC, both in IL and PL subregions (independent samples T-test; IL: $t(12) = 0.42$, $p = .682$, PL: $t(12) = -0.13$, $p = .897$), indicating that no deficits in OLs in the early stages of development are present in APO-SUS rats.

Discussion

This study has provided evidence that interneurons in the mPFC of APO-SUS rats are hypomyelinated compared to those in APO-UNSUS rats, which can be partly rescued by exposing animals to EE during PFC development. We found a lower density of myelinated axons in APO-SUS compared to APO-UNSUS rats, whereas previous research has indicated that total axonal density is the same in APO-SUS and APO-UNSUS rats (Maas et al., unpublished data), meaning that it is a specific defect of myelination. EE did not significantly increase the density of myelinated axons compared to that of APO-SUS rats in standard housing. However, myelinated axon density of the APO-SUS EE group lies between that of the APO-SUS and APO-UNSUS groups with standard housing. EE thus did increase myelinated axon density to such an extent that the significant difference between APO-SUS and APO-UNSUS groups disappeared. Moreover, we found a large increase in myelinated axon density in APO-SUS EE compared to APO-SUS (IL: APO-SUS $M = 13098$, $SD = 5675$, APO-SUS EE $M = 23691$, $SD = 9954$; PL: APO-SUS $M = 12312$, $SD = 4172$, APO-SUS EE $M = 15507$, $SD = 3313$) and combined with the reduced likelihood of finding significance due to the small sample size, we assume EE to have a normalising effect on myelinated axon density. However, since EE does not fully normalise myelinated axon density to APO-UNSUS levels, we conclude that several factors are necessary for a complete rescue. Thus, exercise not only alleviates symptomatology in SZ patients (Mittal et al., 2017) and restores cognitive flexibility in APO-SUS rats (Maas et al., unpublished data), but in addition to that we have shown that EE also positively affects the underlying structure of cognitive symptoms in SZ. These data combined suggest that cognitive, motor, and social stimulation could function as an effective preventive measure against development of SZ in high-risk individuals by making the underlying structure more resilient against drawbacks, or as an addition to or replacement of currently used treatments against the progression of symptoms.

Although the ANOVA for the difference in myelinated axon density was not significant, the effects sizes and relative differences between the APO-SUS and APO-UNSUS groups were to such an extent that we wanted to investigate this further. In addition, the non-significance of the ANOVA could be due to the low power of the test as a result of the rather small sample size. For these reasons, we decided to perform a post-hoc test to shed more light on differences between groups. However, to increase power, it would be good to replicate this experiment with a larger sample size to validate the findings.

While the densities of myelinated axons were significantly different between APO-SUS and APO-UNSUS groups, the integrity of the myelin was normal in all groups. This finding suggests that rather than demyelination, where disintegrated or thin myelin is often observed, hypomyelination occurred, meaning that less axons are myelinated, but the myelin that is produced is of good quality. This finding is supported by previous data indicating that no myelin debris has been found in macrophages in APO-SUS mPFC (Maas et al., unpublished data), and that the myelin deficits occur during adolescence, when myelin in the PFC is maturing, rather than during adulthood, when myelin should be fully developed and thus can be broken down. In the PL subregion of the mPFC, we found a significantly lower G-ratio in APO-UNSUS compared to APO-SUS animals. As the mean G-ratios in IL and the APO-SUS, APO-SUS EE and APO-UNSUS EE G-ratios in PL were all equal, this was a surprising finding which we have not been able to interpret. However, the difference that was found is very small and both mean G-ratios lie in the normal optimal range, suggesting that this difference may not be clinically relevant.

Having shown that reduced WM integrity is a result of hypomyelination rather than demyelination, we assumed that this was caused by a defect in myelinating OLs. Maas et al. (2017) have reported that oxidative stress, which is often found in SZ brains, can cause a deficit in the maturation of oligodendrocyte precursor cells (OPCs). As a result of this, less myelinating OLs are available for myelination of the axons, which could be the cause of hypomyelination. In order to verify that indeed a deficit in myelinating OLs was present, we stained mPFC slices of both APO-SUS and APO-UNSUS animals with anti-BCAS1 antibody, which is a marker present in early myelinating OLs. We expected that fewer myelinating OLs would be present in APO-SUS compared to APO-UNSUS rats. Contrary to our hypothesis, we found no difference in the number of BCAS1-positive cells between APO-SUS and APO-UNSUS mPFC at PND21. To specify more precisely in which stage of proliferation the OLs were, we quantified in PND90 only the premyelinating OLs, containing radial processes. This too indicated no difference between APO-SUS and APO-UNSUS mPFC. These data suggest that defects in early myelinating OLs do not lie at the root of hypomyelination of APO-SUS mPFC. As early myelinating OLs progress further into mature myelinating OLs, where BCAS1 is no longer expressed, it is probable that differences can be found in this further progressed stage. Therefore, it would be good to replicate this experiment with markers for both stages of myelinating OLs. Unfortunately, this was beyond the scope of this project.

To determine more precisely where the reduction in myelinated axons in APO-SUS mPFC originated from, we performed a distribution analysis of the axon calibres of the myelinated axons per group. As myelin thickness varies with axon calibre, it is probable that axons of a certain size are particularly vulnerable to hypomyelination. With a Kolmogorov-Smirnov test, we found no significant difference in location and shape between the distributions of the four groups. However, as we had previously found, and what can also be observed in the distributions (Figure 2), there was a difference in the total number of myelinated axons, suggesting that the effects that we found are general and not attributable to a specific axon calibre. Likewise, EE has a general positive effect on the number of myelinated axons in APO-SUS mPFC. Axons with different calibres are therefore all equally vulnerable to hypomyelination.

As axon calibre was not a determining factor in which axons would be myelinated, another factor was investigated, namely the functional type of axon. The interneuron subtype was of interest in this context due to its importance in neuronal synchronisation necessary for cognitive functioning, and because of its found alterations associated with SZ. We were mainly interested

in the PV-positive subtype of interneuron, but it proved to be very difficult to stain for PV. Therefore, we chose to use an antibody against GABA, staining all interneurons, including the PV-positive ones. Considering the finding that the PV subclass of interneurons is the main type of interneuron that is myelinated (Micheva et al., 2016; 2018), we assumed myelinated GABA-positive axons to be of the PV subclass, making a GABA staining a suitable alternative to a PV staining. However, as we did not stain directly for PV, we can only draw conclusions about myelination of interneurons in general rather than about the PV-positive subclass specifically. As the most pronounced differences had been found in the IL subarea in previous analyses, we only analysed this area for the current experiment. When comparing the total myelinated axon density and the GABAergic myelinated axon density between APO-SUS and APO-UNSUS rats, we see that APO-SUS has slightly lower densities in both measures, although both the analyses did not reach significance. As the lower density of GABAergic myelinated axons in APO-SUS could be due to the lower density of total myelinated axons, we normalised for the total myelinated axon density by calculating the percentage of myelinated axons that contain GABA. This showed us that indeed there is a significantly lower percentage of GABAergic myelinated axons in APO-SUS as compared to APO-USNUS PFC. These data are a strong first indication that indeed the GABAergic interneuron specifically is hypomyelinated in APO-SUS rats. However, hypomyelination of the GABAergic interneuron does not account for the total reduction in myelinated axons, suggesting that it is not the only type of interneuron that is hypomyelinated. Dopamine has already been implicated with SZ for a long time, and recently, cortical deficits of dopaminergic neurotransmission have been found to be an important factor in SZ symptomatology (Howes & Kapur, 2009). Additionally, abnormalities in prefrontal glutamate transmission have also been associated with SZ (Laruelle et al., 2003). In future research, it would therefore be interesting to investigate not only hypomyelination of interneurons, but also of dopaminergic and glutamatergic neurons.

Throughout the data collection and analysis, we have handled IL and PL subareas of the mPFC separately. Often the effect was only or most strongly to be found in the IL area. This could be explained by the possibly different cortical layers that our images were taken in. We took images at approximately 300 μm from the corpus callosum in both IL and PL subareas. In the IL area this distance led us just into layer 5 of the cortex, but as the PL area appears to have a thicker cortical layer 6 (Perez-Cruz et al., 2007), we possibly arrived in layer 6 rather than layer 5 in the PL area. The different cortical layers could therefore explain the differences in results between IL and PL.

Limitations of the study

The main limitation of the current research is the sample size of the experimental animal groups. The ideal sample size was calculated to detect our expected effect size, but as we worked with animals, it was important not to use more animals than necessary. Unfortunately, difficulties in the processing of some samples were encountered, causing these samples to be no longer suitable for analysis. Therefore, the sample sizes available for analysis were in a number of cases smaller than the calculated optimal sample size, increasing the chance of finding false negatives. Although this problem will always be present in animal studies, the results of our study would be more conclusive if they were replicated with a larger number of animals.

Another limitation is that we could only stain for the total set of GABAergic interneurons, while our goal was to shed light on the myelination of PV-positive interneurons specifically. As was mentioned above, a GABA staining was the best option considering the current possibilities, but to draw more concrete conclusions, it would be best to replicate the study with an antibody against PV rather than against GABA.

Additionally, in retrospect it seems like the BCAS1 antibody was not the best choice for determining during which stage of OL development defects might arise. Although Fard et al. (2017) suggest that the BCAS1-protein is mainly present in early myelinating OLs, it is also observed in OPCs. The BCAS1-protein is thus not as specific for one stage of OL development as we initially thought. In order to test the hypothesis that maturation of OPCs into mature OLs halts along the way, and to know more precisely in which stage this halt occurs, it would be beneficial to find markers that are more specific to the separate stages of OL development.

Lastly, considering that we possibly analysed images from two different cortical layers in the PL and IL areas, we cannot draw decisive conclusions on different effects occurring in PL and IL, as they could also be attributable to the different layers the data was collected from. For the current study this was not a problem, but for future research it would be desirable to verify that the same layer is analysed in PL and IL areas.

Conclusion

In this study we have shown that there are significant differences in the density of myelinated axons in mPFC between APO-SUS and APO-UNSUS animals. We have found strong indications that environmental enrichment has a normalising effect on this measure. The hypomyelination effect is found to be a general effect for all axon calibres, but it is shown that interneurons specifically are affected by hypomyelination. Our data indicate that the hypomyelination in APO-SUS mPFC is not due to a decreased density of early myelinating oligodendrocytes, while it could be due to a lower density of mature myelinating oligodendrocytes. These data contribute to a more profound understanding of the neurobiological mechanisms underlying cognitive symptoms in schizophrenia. However, future research could contribute to the current knowledge by focusing on acquiring a more extensive overview of which functional types of neurons are vulnerable to hypomyelination. Additionally, a necessary next step for the translation of these results to schizophrenia patients, is to replicate the findings in healthy human tissue and tissue of schizophrenia patients.

Acknowledgements

I would like to thank Dorien Maas, MSc, for her continuous help and guidance with the project, and Prof. Gerard Martens and Dr. Brahim Nait-Oumesmar for opening their labs to me and their guidance throughout the project. I would like to thank Dr. Dominique Langui and Asha Baskaran (ICM-Quant, Institut du Cerveau et de la Moelle épinière, Paris, France) for their advice and help with electron microscopy, and all employees of the Department of Molecular Animal Physiology (Radboud Institute for Molecular Life Sciences, Radboudumc, Radboud University Nijmegen, the

Netherlands) and the Department of Myelin Plasticity and Repair (Institut du Cerveau et de la Moelle épinière, Paris, France) for welcoming me into their lab and assisting me when needed.

References

Akbarian, S., Kim, J. J., Potkin, S. G., Hagman, J. O., Tafazzoli, A., Bunney, W. E., & Jones, E. G. (1995). Gene expression for glutamic acid decarboxylase is reduced without loss of neurons in prefrontal cortex of schizophrenics. *Archives of general psychiatry*, *52*(4), 258-266.

Benes, F. M., McSparren, J., Bird, E. D., SanGiovanni, J. P., & Vincent, S. L. (1991). Deficits in small interneurons in prefrontal and cingulate cortices of schizophrenic and schizoaffective patients. *Archives of general psychiatry*, *48*(11), 996-1001.

Breier, A., Buchanan, R. W., Elkashef, A., Munson, R. C., Kirkpatrick, B., & Gellad, F. (1992). Brain morphology and schizophrenia: a magnetic resonance imaging study of limbic, prefrontal cortex, and caudate structures. *Archives of general psychiatry*, 49(12), 921-926.

Buchanan, R. W., Vladar, K., Barta, P. E., & Pearlson, G. D. (1998). Structural evaluation of the prefrontal cortex in schizophrenia. *American Journal of Psychiatry*, 155(8), 1049-1055.

Chang, E. H., Argyelan, M., Aggarwal, M., Chandon, T. S. S., Karlsgodt, K. H., Mori, S., & Malhotra, A. K. (2017). The role of myelination in measures of white matter integrity: combination of diffusion tensor imaging and two-photon microscopy of CLARITY intact brains. *Neuroimage*, 147, 253-261.

Do, K. Q., Cuenod, M., & Hensch, T. K. (2015). Targeting oxidative stress and aberrant critical period plasticity in the developmental trajectory to schizophrenia. *Schizophrenia bulletin, 41*(4), 835-846.

Fard, M. K., van der Meer, F., Sánchez, P., Cantuti-Castelvetri, L., Mandad, S., Jäkel, S., ... & Kuhlmann, T. (2017). BCAS1 expression defines a population of early myelinating oligodendrocytes in multiple sclerosis lesions. *Science translational medicine*, *9*(419), eaam7816.

Flynn, S. W., Lang, D. J., Mackay, A. L., Goghari, V., Vavasour, I. M., Whittall, K. P., ... & Falkai, P. (2003). Abnormalities of myelination in schizophrenia detected in vivo with MRI, and post-mortem with analysis of oligodendrocyte proteins. *Molecular psychiatry*, *8*(9), 811.

Filiou, M. D., Teplytska, L., Otte, D. M., Zimmer, A., & Turck, C. W. (2012). Myelination and oxidative stress alterations in the cerebellum of the G72/G30 transgenic schizophrenia mouse model. *Journal of psychiatric research*, 46(10), 1359-1365.

Fitzsimmons, J., Kubicki, M., & Shenton, M. E. (2013). Review of functional and anatomical brain connectivity findings in schizophrenia. *Current opinion in psychiatry*, 26(2), 172-187.

Fraher, J., & Dockery, P. (1998). A strong myelin thickness-axon size correlation emerges in developing nerves despite independent growth of both parameters. *The Journal of Anatomy*, *193*(2), 195-201.

Gonzalez-Burgos, G., Cho, R. Y., & Lewis, D. A. (2015). Alterations in cortical network oscillations and parvalbumin neurons in schizophrenia. *Biological psychiatry*, *77*(12), 1031-1040.

Gonzalez-Burgos, G., & Lewis, D. A. (2008). GABA neurons and the mechanisms of network oscillations: implications for understanding cortical dysfunction in schizophrenia. *Schizophrenia bulletin, 34*(5), 944-961.

Green, M. F. (2006). Cognitive impairment and functional outcome in schizophrenia and bipolar disorder. *The Journal of clinical psychiatry*, *67*, 3-8.

Gregg, J. R., Herring, N. R., Naydenov, A. V., Hanlin, R. P., & Konradi, C. (2009). Downregulation of oligodendrocyte transcripts is associated with impaired prefrontal cortex function in rats. *Schizophrenia research*, *113*(2-3), 277-287.

Hakak, Y., Walker, J. R., Li, C., Wong, W. H., Davis, K. L., Buxbaum, J. D., ... & Fienberg, A. A. (2001). Genome-wide expression analysis reveals dysregulation of myelination-related genes in chronic schizophrenia. *Proceedings of the National Academy of Sciences*, *98*(8), 4746-4751.

Haroutunian, V., Katsel, P., Dracheva, S., & Davis, K. L. (2006). The human homolog of the QKI gene affected in the severe dysmyelination "quaking" mouse phenotype: downregulated in multiple brain regions in schizophrenia. *American Journal of Psychiatry*, *163*(10), 1834-1837.

Hashimoto, T., Volk, D. W., Eggan, S. M., Mirnics, K., Pierri, J. N., Sun, Z., ... & Lewis, D. A. (2003). Gene expression deficits in a subclass of GABA neurons in the prefrontal cortex of subjects with schizophrenia. *Journal of Neuroscience*, *23*(15), 6315-6326.

Hof, P. R., Haroutunian, V., Copland, C., Davis, K. L., & Buxbaum, J. D. (2002). Molecular and cellular evidence for an oligodendrocyte abnormality in schizophrenia. *Neurochemical research*, *27*(10), 1193-1200.

Howes, O. D., & Kapur, S. (2009). The dopamine hypothesis of schizophrenia: version III—the final common pathway. *Schizophrenia bulletin*, *35*(3), 549-562.

Kann, O., Papageorgiou, I. E., & Draguhn, A. (2014). Highly energized inhibitory interneurons are a central element for information processing in cortical networks. *Journal of Cerebral Blood Flow & Metabolism*, *34*(8), 1270-1282.

Karlsgodt, K. H., van Erp, T. G., Poldrack, R. A., Bearden, C. E., Nuechterlein, K. H., & Cannon, T. D. (2008). Diffusion tensor imaging of the superior longitudinal fasciculus and working memory in recent-onset schizophrenia. *Biological psychiatry*, *63*(5), 512-518.

Kooyman, I., Dean, K., Harvey, S., & Walsh, E. (2007). Outcomes of public concern in schizophrenia. British Journal of Psychiatry, 191(S50), S29-S36. doi:10.1192/bjp.191.50.s29

Kubicki, M., McCarley, R. W., & Shenton, M. E. (2005). Evidence for white matter abnormalities in schizophrenia. *Current opinion in psychiatry*, *18*(2), 121.

Kuswanto, C. N., Teh, I., Lee, T. S., & Sim, K. (2012). Diffusion tensor imaging findings of white matter changes in first episode schizophrenia: a systematic review. *Clinical Psychopharmacology and Neuroscience*, *10*(1), 13.

Laruelle, M., Kegeles, L. S., & Abi-Dargham, A. (2003). Glutamate, dopamine, and schizophrenia. *Annals of the New York Academy of Sciences*, *1003*(1), 138-158.

Lewis, D. A. (2009). Neuroplasticity of excitatory and inhibitory cortical circuits in schizophrenia. *Dialogues in clinical neuroscience*, *11*(3), 269.

Lewis, D. A., Curley, A. A., Glausier, J. R., & Volk, D. W. (2012). Cortical parvalbumin interneurons and cognitive dysfunction in schizophrenia. *Trends in neurosciences, 35*(1), 57-67.

Micheva, K. D., Chang, E. F., Nana, A. L., Seeley, W. W., Ting, J. T., & Cobbs, C. (2018). Distinctive Structural and Molecular Features of Myelinated Inhibitory Axons in Human Neocortex. *eNeuro*, *5*(5).

Micheva, K. D., Wolman, D., Mensh, B. D., Pax, E., Buchanan, J., Smith, S. J., & Bock, D. D. (2016). A large fraction of neocortical myelin ensheathes axons of local inhibitory neurons. *Elife*, *5*, e15784.

Mittal, V. A., Vargas, T., Osborne, K. J., Dean, D., Gupta, T., Ristanovic, I., ... & Shankman, S. A. (2017). Exercise treatments for psychosis: a review. *Current treatment options in psychiatry, 4*(2), 152-166.

Orellana, G., & Slachevsky, A. (2013). Executive functioning in schizophrenia. *Frontiers in Psychiatry*, 4. doi:10.3389/fpsyt.2013.00035

Pajevic, S., Basser, P. J., & Fields, R. D. (2014). Role of myelin plasticity in oscillations and synchrony of neuronal activity. *Neuroscience*, *276*, 135-147.

Perez-Cruz, C., Müller-Keuker, J. I., Heilbronner, U., Fuchs, E., & Flügge, G. (2007). Morphology of pyramidal neurons in the rat prefrontal cortex: lateralized dendritic remodeling by chronic stress. *Neural plasticity*, *2007*.

Prata, D. P., Kanaan, R. A., Barker, G. J., Shergill, S., Woolley, J., Georgieva, L., ... & Toulopoulou, T. (2013). Risk variant of oligodendrocyte lineage transcription factor 2 is associated with reduced white matter integrity. *Human brain mapping*, *34*(9), 2025-2031.

Qiu, A., Zhong, J., Graham, S., Chia, M. Y., & Sim, K. (2009). Combined analyses of thalamic volume, shape and white matter integrity in first-episode schizophrenia. Neuroimage, *47*(4), 1163-1171.

Reichenberg, A., Caspi, A., Harrington, H., Houts, R., Keefe, R., Murray, R., ... & Moffitt, T. (2010). Static and dynamic cognitive deficits in childhood precede adult schizophrenia: a 30-year study. *Schizophrenia Research*, *2*(117), 175.

Reichenberg, A., Weiser, M., Caspi, A., Knobler, H. Y., Lubin, G., Harvey, P. D., ... & Davidson, M. (2006a). Premorbid intellectual functioning and risk of schizophrenia and spectrum disorders. *Journal of clinical and experimental neuropsychology*, *28*(2), 193-207.

Reichenberg, A., Weiser, M., Rapp, M. A., Rabinowitz, J., Caspi, A., Schmeidler, J., ... & Davidson, M. (2006b). Premorbid intra-individual variability in intellectual performance and risk for schizophrenia: a population-based study. *Schizophrenia research*, *85*(1-3), 49-57.

Rosenbluth, J., & Bobrowski-Khoury, N. (2013). Structural bases for central nervous system malfunction in the quaking mouse: dysmyelination in a potential model of schizophrenia. *Journal of neuroscience research*, 91(3), 374-381.

Saha, S., Chant, D., Welham, J., & McGrath, J. (2005). A systematic review of the prevalence of schizophrenia. *PLoS medicine*, 2(5), e141.

Scheel, M., Prokscha, T., Bayerl, M., Gallinat, J., & Montag, C. (2013). Myelination deficits in schizophrenia: evidence from diffusion tensor imaging. *Brain Structure and Function*, 218(1), 151-156.

Stedehouder, J., & Kushner, S. A. (2017). Myelination of parvalbumin interneurons: a parsimonious locus of pathophysiological convergence in schizophrenia. *Molecular psychiatry*, *22*(1), 4.

Tomlinson, L., Leiton, C. V., & Colognato, H. (2016). Behavioral experiences as drivers of oligodendrocyte lineage dynamics and myelin plasticity. *Neuropharmacology*, *110*, 548-562.

Volk, D. W., Austin, M. C., Pierri, J. N., Sampson, A. R., & Lewis, D. A. (2000). Decreased glutamic acid decarboxylase67 messenger RNA expression in a subset of prefrontal cortical γ-aminobutyric acid neurons in subjects with schizophrenia. *Archives of general psychiatry*, *57*(3), 237-245.

Voineskos, A. N., Felsky, D., Kovacevic, N., Tiwari, A. K., Zai, C., Chakravarty, M. M., ... & Pollock, B. G. (2012). Oligodendrocyte genes, white matter tract integrity, and cognition in schizophrenia. *Cerebral cortex*, *23*(9), 2044-2057.

Vostrikov, V. M., Uranova, N. A., Rakhmanova, V. I., & Orlovskaia, D. D. (2004). Lowered oligodendroglial cell density in the prefrontal cortex in schizophrenia. *Zhurnal nevrologii i psikhiatrii imeni SS Korsakova*, *104*(1), 47-51.

Xiu, Y., Kong, X. R., Zhang, L., Qiu, X., Chao, F. L., Peng, C., ... & Tang, Y. (2014). White Matter Injuries Induced by MK-801 in a Mouse Model of Schizophrenia Based on NMDA Antagonism. *The Anatomical Record*, *297*(8), 1498-1507.

Yang, S., Li, C., Qiu, X., Zhang, L., Lu, W., Chen, L., ... & Tang, Y. (2013). Effects of an enriched environment on myelin sheaths in the white matter of rats during normal aging: A stereological study. *Neuroscience, 234*, 13-21.